Int. J. Electrochem. Sci., 17 **(2022)** Article Number: 221035, doi: 10.20964/2022.10.02

International Journal of
ELECTROCHEMICAL
SCIENCE
www.electrochemsci.org

Electrochemical Sensor for Highly Sensitive Detection of Gallic Acid Based on Graphitized and Carboxylated Multi-Walled Carbon Nanotubes modified Glassy Carbon Electrode

Gan Zhu, Qian Wang, Yunhang Liu, Meimei Guo, Runqiang Liu[*], *Hongyuan Zhao*[*]

Henan Institute of Science and Technology, Xinxiang 453003, China
[*]E-mail: liurunqiang1983@126.com, hongyuanzhao@126.com

Received: 9 July 2022 / *Accepted:* 7 August 2022 / *Published:* 10 September 2022

Herein, we used the graphitized and carboxylated multi-walled carbon nanotubes (GCMCNTs) to decorate the glass carbon electrode (GCE), which was employed to construct the GCMCNTs/GCE sensor for the detection of GA. GCMCNTs with one-dimensional nanotube-like structure exhibited high specific surface area and excellent electrical conductivity. GCMCNTs with high graphitization degree and carboxylation groups provided more microsites for electrochemical reaction and highly efficient electron transport channels, which helped promote the electron transmission and enhance the dispersibility of carbon material. The GCMCNTs/GCE sensor achieved the sensitive electrochemical determination of GA. The fabricated sensor presented a quite low limit of detection of 0.0032 μM (S/N=3) with the corresponding linear equation of I_p (μA) =21.506C+3.134 (R^2=0.995) in the linear GA concentration range of 0.01-10 μM. In addition, the good GA detection could be realized in the tap water sample.

Keywords: Gallic acid; Electrochemical detection; Graphitization; Carboxylation; Multi-walled carbon nanotubes; Synergistic effect

1. INTRODUCTION

Gallic acid (GA) exists widely in black tea, green tea, grape, blueberry, banana, and other natural plants. It has many advantages such as anti-cancer, anti-mutagenic and anti-oxidant [1-6]. Moreover, it also has strong antiradical activity and electrochemical oxidation effect [7]. It is often used as an additive in food industry, chemical industry and cosmetics industry [8, 9]. However, it has been reported that GA residue in water may pollute the environment due to the low degradability [2]. Therefore, it is significant to design the simple and efficient analytical techniques for the determination of GA.

At present, GA detection mainly depends on several traditional detection methods such as CL, TLC, FIA, HPLC, and UHPLC-MS/MS [9-14]. These analytical techniques have some obvious

disadvantages such as complicated sample process, high analysis cost, complicated steps. The corresponding analytical instruments need professional and technical workers to complete the analysis experiments. It is worth to note that the electrochemical sensing detection technology can overcome these shortcomings. According to the existing literatures [15, 16], the applied voltage realizes the conversion of GA into semiquinone radical, and the further irreversible redox reaction converts the semiquinone radical into quinine through.

The electrochemical sensing detection property can be significantly improved by decorating the surface of glassy carbon electrode (GCE) with carbon materials [17-20]. Huang et al. prepared a Ce-MOF/CNTs sensor to detect hydroquinone (HQ) and its isomer of catechol (CC). The fabricated sensor showed the limit of detection of 5.3 μM and 3.5 μM (S/N=3) in the corresponding linear ranges of 10-100 μM and 5-50 μM, respectively [21]. Winiarski et al. fabricated the f-MWCNT-$Ni(OH)_2$-$Si_4Pic^+Cl^-$/GCE sensor for the determination of folic acid (FA), which achieved a limit of detection of 0.095 μM (S/N=3) in a widely linear range from 0.5 μM to 26 μM [22]. In addition, Zhao et al. modified the GCE surface by using the nanocomposite of carbon nanotubes and carbon nanosheets for the fabrication of 3D IPCNT/CNS/GCE sensor, which showed a low limit of detection is 0.016 μM in the linear segments of 0.05-20 μM [1]. It can be concluded that carbon materials have a very important impact on improving the detection performance of electrochemical sensors.

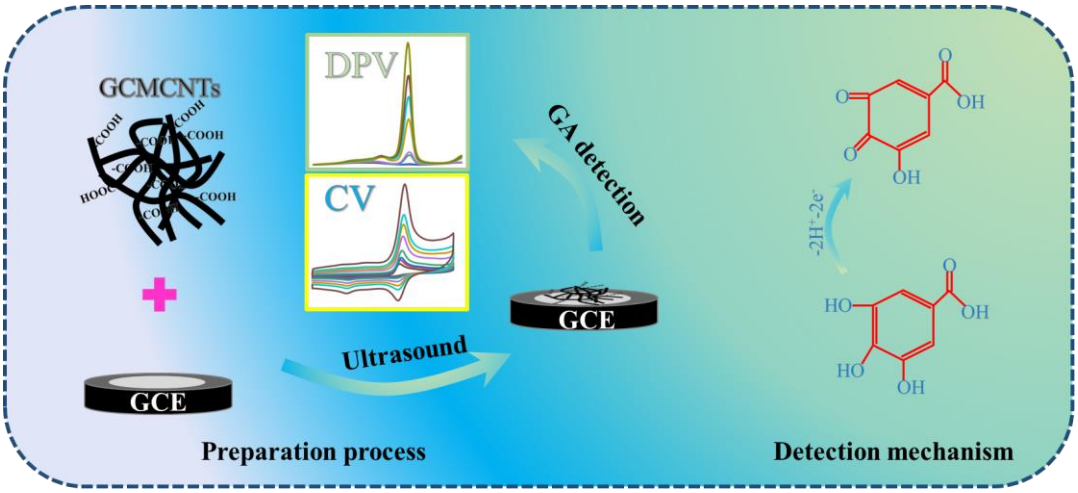

Scheme 1. Fabrication of the GCMCNTs/GCE sensor for the GA determination.

Herein, the graphitized and carboxylated multi-walled carbon nanotubes (GCMCNTs) to decorate the glass carbon electrode (GCE), which was employed to construct the GCMCNTs/GCE sensor for the detection of GA, as shown in **Scheme 1**. GCMCNTs with one-dimensional nanotube-like structure exhibited high specific surface area and excellent electrical conductivity. GCMCNTs with high graphitization degree and carboxylation groups provided more microsites for electrochemical reaction and highly efficient electron transport channels, which helped promote the electron transmission and enhance the dispersibility of carbon material [23, 24]. The GCMCNTs/GCE sensor achieved the sensitive electrochemical determination of GA.

2. EXPERIMENTAL

2.1. Materials and reagents

Graphitized and carboxylated multi-walled carbon nanotubes (GCMCNTs, >99.9%), sodium phosphate dibasic (Na_2HPO_4, AR, 99%), nitric acid (HNO_3, 65-68 wt.% in H_2O), sodium dihydrogen phosphate (NaH_2PO_4, AR, 99%), dimethylformamide (DMF, AR, 99.5%), hydrochloric acid (HCL, 37%) and ethanol (CH_3CH_2OH, AR,95.0%).

2.2. Preparation of GCMCNTs/GCE

The GCMCNTs/GCE sensor was prepared by the drip coating method. In a typical process, 10 mg of GCMCNTs was weighed and further dispersed in 5 mL of DMF solution. After ultrasonic treatment for one hour, the black GCMCNTs suspension obtained to prepare the electrochemical sensor. Before the GCMCNTs/GCE sensor, the GCE surface was polished by using the abrasive alumina with different particle sizes. And then, the pretreated GCE surface was further washed by ultrasound method in deionized water and alcohol solution. Finally, the GCMCNTs/GCE sensor was fabricated by dripping 5 μL of the black GCMCNTs suspension onto the clean GCE surface followed with the dried process with the help of infrared ray lamp.

2.3. Characterization and measurements

The surface morphology of modification material can play an imported role on the electrochemical sensing detection performance. GCMCNTs were observed by transmission electron microscope (TEM) to confirm the surface morphology and microstructure. The electrochemical determination performance of GA was performed by electrochemical impedance spectroscopy (EIS), cyclic voltammetry (CV) and differential pulse voltammetry (DPV). In order to improve the GA sensitivity and analytical efficiency, the effect of GA accumulation time on the detection property was tested by DPV measurement. Before starting the DPV measurement, the working electrode needs to be immersed in the electrolyte for some time, which can be carried out by adjusting the parameter of deposition time.

3. RESULTS AND DISCUSSION

3.1 Physical characterization of GCMCNTs

Fig. 1 shows the TEM images of the GCMCNTs sample. It is obvious that the GCMCNTs sample has one-dimensional nanotube-like structure. The intertwined conductive carbon structures of GCMCNTs can provide more microsites for electrochemical reaction and highly efficient electron transport channels, which help promote the electron transmission and enhance the dispersibility of carbon material [25-27].

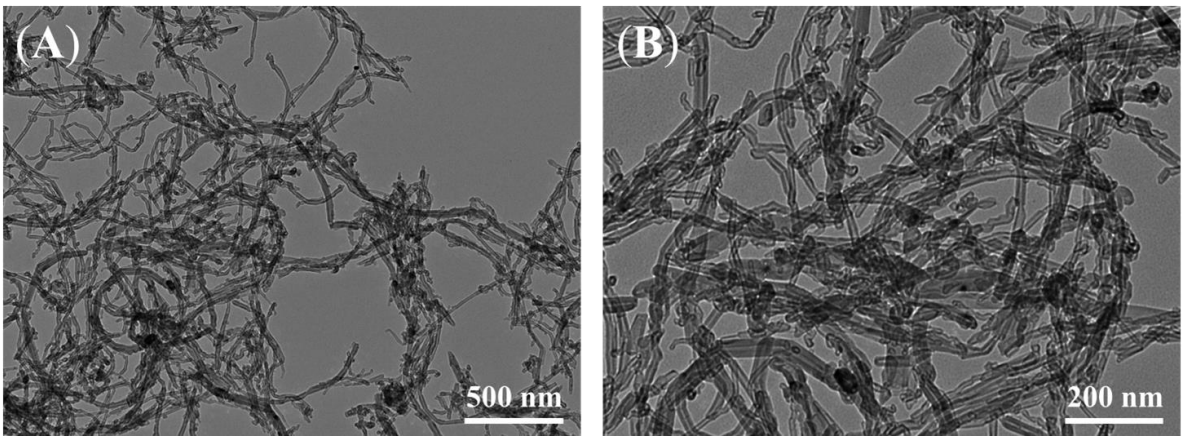

Figure 1. TEM images of the GCMCNTs sample.

3.2 Electrochemical characterization

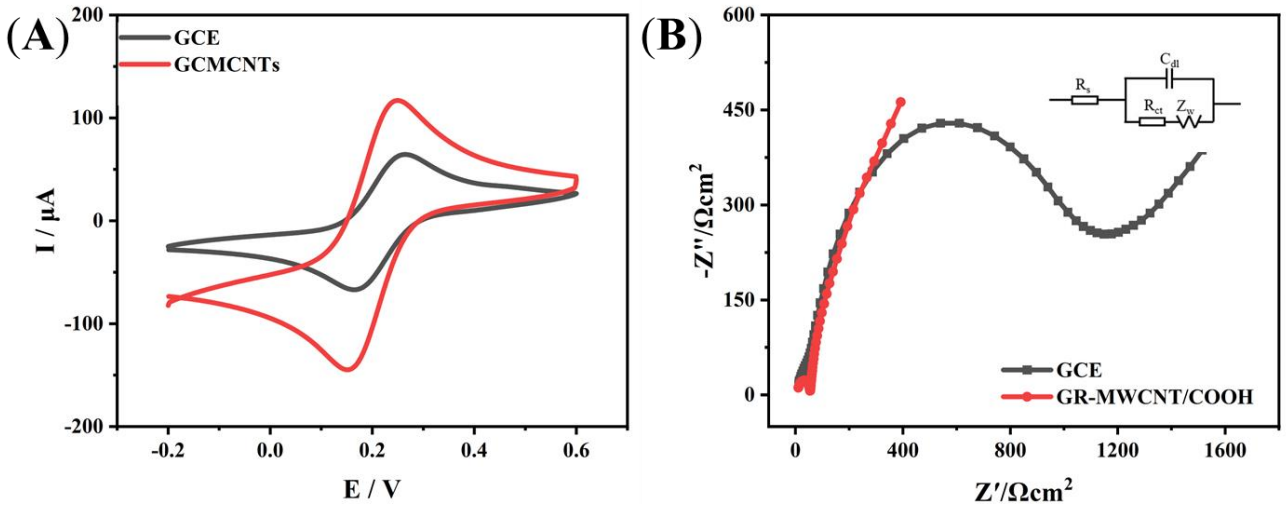

Figure 2. (A) CV curves and (B) Nyquist plots of the undecorated GCE and GCMCNTs/GCE sensors (Solution: 5 mM $[Fe(CN)_6]^{3-/4-}$ dissolved in 0.1 M KCl).

Fig. 2 shows the electrochemical characterization results of the undecorated GCE and GCMCNTs/GCE sensors based on the CV measurement. As shown in **Fig. 2(A)**, the electrochemical performance could be significantly improved by the modification of GCMCNTs. It is obvious that the GCMCNTs/GCE sensor has higher peak currents compared to the undecorated GCE sensor. **Fig. 2(B)** exhibits the Nyquist plots of the undecorated GCE and GCMCNTs/GCE sensors. Based on the analysis results, the R_{ct} of undecorated GCE sensor is 1111.38 Ω cm^2. By contrast, the R_{ct} of GCMCNTs/GCE sensor is smaller (48.07 Ω cm^2), which suggests the excellent conductivity property of GCMCNTs [24-28].

3.3 Study on electrochemical behavior

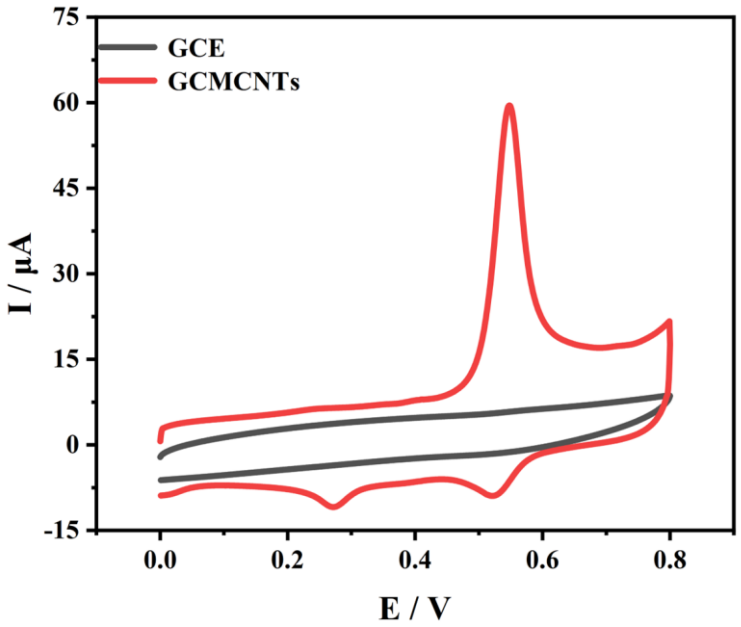

Figure 3. CV curves of 10 μM GA at the undecorated GCE and GCMCNTs/GCE sensors (Parameters: pH=1.0, solution: 10 μM GA, scan rate: 100 mV s^{-1}, potential range: 0-0.8 V).

Fig. 3 presents the determination performance of 10 μM GA at the undecorated GCE and GCMCNTs/GCE sensors. As shown here, the CV curve of the bare GCE is smooth. By contrast, the CV curve of GCMCNTs/GCE sensor has clear reversible redox peaks with high anode peak current of 47.16 μA. Such good GA determination performance has much to do with the excellent electrical conductivity, enough specific surface area, good hydrophilicity of GCMCNTs with one-dimensional nanotube-like structure [16-18]. GCMCNTs with high graphitization degree and carboxylation groups provided more microsites for electrochemical reaction and highly efficient electron transport channels, which helps promote the electron transmission and enhance the dispersibility of carbon material [23, 29].

3.4 Effect of experiment conditions

3.4.1 Effect of pH

Fig. 4(A-C) provide the impact of pH value on the MP detection performance of the GCMCNTs/GCE sensor with the help of DPV curves. It is worth to note that the peak value gradually increases with the decrease of pH in the range of 5.0-1.0, which agrees with the existing literature [16, 30-35]. Therefore, the pH=1.0 was applied as the optimal pH value for the GA determination. **Fig. 4(C)** exhibits the change relationship of peak potential value with pH value. The peak potential value gradually decreases with the increase of pH in the range of 1.0-5.0, which can be confirmed by the corresponding fitting equation is E_{pa}=-0.064pH+0.569 (R^2=0.995). And it is significant to note that the linear fitting relationship presents a slope value of 64 mV/pH, which indicating that the transfer of electron and proton in the GA electrochemical reaction at the GCMCNTs/GCE sensor is equal [30, 31].

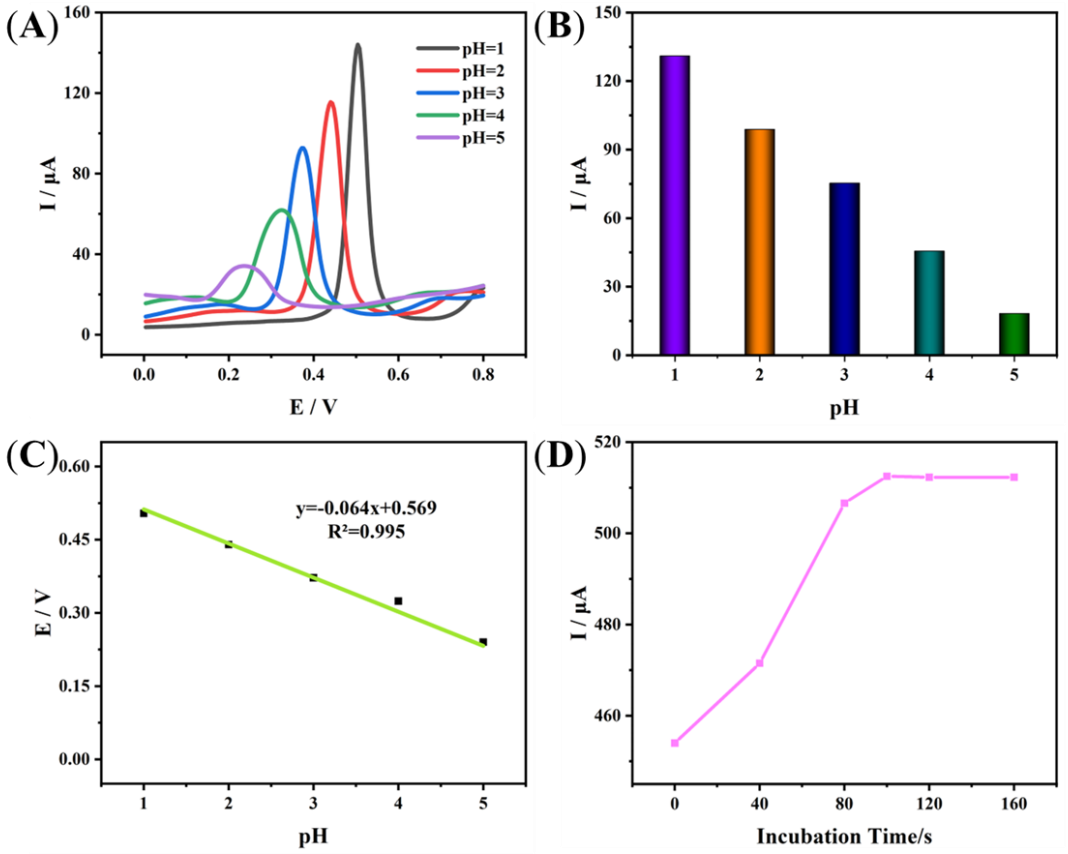

Figure 4. (A) DPV curves of 10 μM GA at the GCMCNTs/GCE sensor, (B) change relationship of peak current with pH value, (C) fitting relationship of peak potential and pH value (pH: 1.0-5.0, solution: 10 μM GA, potential range: 0-0.8 V), and (D) change relationship of peak current with accumulation time (Parameters: pH=1.0, solution: 50 μM GA).

3.4.2 Effect of accumulation time

Fig. 4(D) presents the impact of incubation time on the DPV curves of 50 μM GA at the GCMCNTs/GCE sensor. It can be seen that the peak value gradually increases with the decrease of the accumulation time. The peak value reaches the maximum value as the accumulation time reaches up to 100 seconds. And the peak value remains unchanged with the increase of the accumulation time after 100 seconds. Thus, the accumulation time can be set to be 100s for the efficient GA detection.

3.4.3 Effect of scan rate

In order to further explore the GA analysis performance of the GCMCNTs/GCE sensor based on the CV curves at different scanning rates of 10-300 mV/s, as shown in **Fig. 5(A)**. It is important to note that the peak value gradually increases with the increase of scanning rate. **Fig. 5(B)** presents the fitting relationship of peak current value with scanning rate. The corresponding linear fitting equation is I_p (μA) =0.286v+12.688 (R^2=0.996), indicating that the electrochemical reaction of GA at the GCMCNTs/GCE sensor is an adsorption-controlled process [29-31].

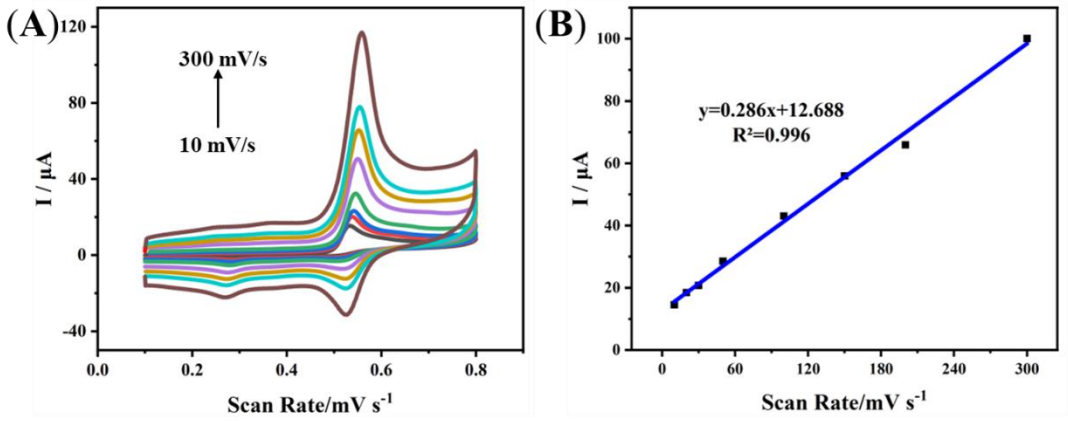

Figure 5. (A) Effect of scanning rate on the CV curve of 10 μM GA at the GCMCNTs/GCE sensor and (B) fitting relationship of peak current value with scanning rate (Parameters: pH=1, solution: 10 μM GA, scan rate range: 10-300 mV s^{-1}, potential range: 0-0.8 V).

3.5 Analytical performance

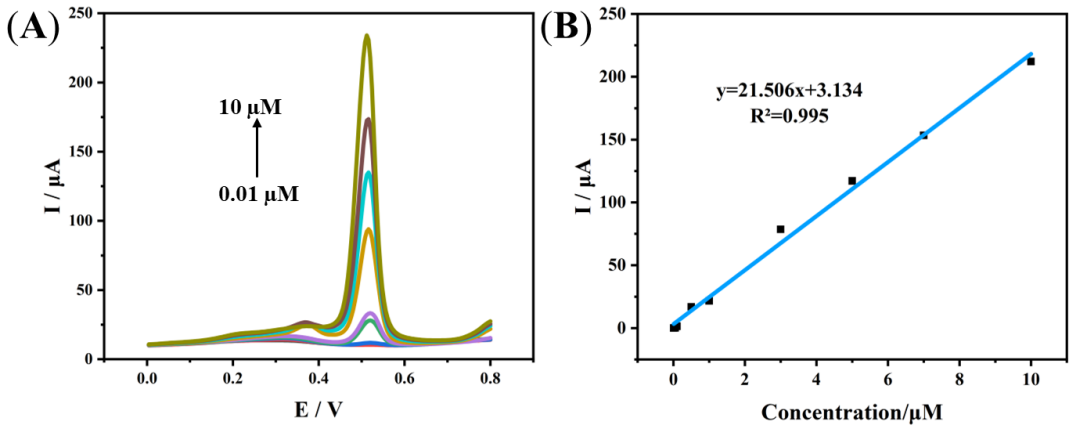

Figure 6. (A) Effect of GA concentration on the DPV curves of GA at the GCMCNTs/GCE sensor and (B) fitting relationship of peak value with GA concentration (Parameters: pH=1, GA concentration: 0.01-10 μM, deposition time: 100s, potential range: 0-0.8 V).

Fig. 6(A) shows the effect of GA concentration on the DPV curves of GA at the GCMCNTs/GCE sensor under the optimal experimental conditions, and the change range of GA concentration is 0.01-10 μM (including 0.01, 0.05, 0.1, 0.5, 1, 3, 5, 7 and 10 μM). As can be seen, the peak value gradually increases with the increase of GA concentration. **Fig. 6(B)** exhibits the fitting relationship of peak value with GA concentration. The corresponding linear fitting equation is I_p (μA) =21.506C+3.134 (R^2=0.995), which achieved a low limit of detection of 0.0032 μM (S/N=3). The fabricated sensor showed satisfactory GA detection performance, which mainly benefited from the GCMCNTs sample with high graphitization degree and carboxylation groups provided more microsites for electrochemical reaction and highly efficient electron transport channels, which helps promote the electron transmission and enhance the dispersibility of carbon material [23-28]. **Table 1** lists the GA electrochemical analysis

performance of different electrochemical sensors. Compared with other reported GA sensors, the fabricated GCMCNTs/GCE sensor shows excellent electrochemical analysis performance for the detection of GA, and the fabricated sensor does not involve the complicated experimental steps. Especially, the GCMCNTs/GCE sensor can show a lower detection limit than that of the previously reported sensor, which suggests that the further graphitization can contribute to the more sensitive GA detection performance.

Table 1. The determination performance of GA at different electrochemical sensors.

Electrode materials	Limit of detection (μM)	Range of linear (μM)	Reference
ZrO_2NPs-AuNPs- DES/CPE	0.025	0.22-55	[36]
MOF-801/MC-3/GCE	0.15	0.2-5, 5-100	[37]
AgNP/Delph/GCE	0.28	0.60-8.68, 8.68-625.80	[9]
SPCE/PME	0.210	1-1000	[38]
RGO-CCE	0.0867	0.51-46.46	[6]
SiO_2/CPE	0.25	0.8-100	[39]
GCMCNTs/GCE	0.0032	0.01-10	This work

3.6 Reproducibility, repeatability, and selectivity of GCMCNTs/GCE

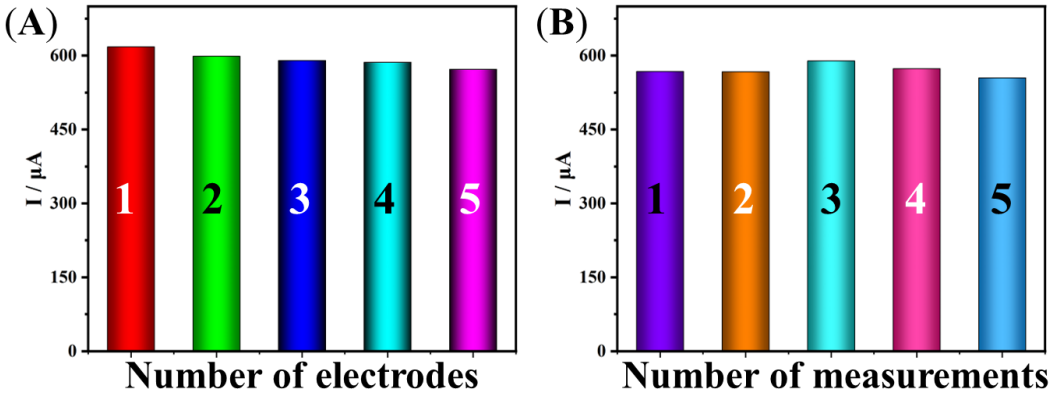

Figure 7. (A) Reproducibility and (B) repeatability of the GCMCNTs/GCE sensor (Parameters: pH=1, solution: 50 μM GA, deposition time: 100s).

Fig. 7(A) provides the results of reproducibility measurement based on five different GCMCNTs/GCE electrodes. It can be seen that the GCMCNTs/GCE sensor presents the good reproducibility with relative standard deviation (RSD) value of 2.82%. **Fig. 7(B)** exhibits the results of repeatability measurement based on five different measurements at the same GCMCNTs/GCE sensor. It is obvious the difference between these peak currents is very small with relative standard deviation (RSD) value of 2.19%, which suggests the excellent repeatability. **Fig. 8** shows the result of selectivity of GCMCNTs/GCE for the GA determination. The interfering substances involve glucose, Na^+, K^+, Mg^{2+}, Cu^{2+}, Zn^{2+}, and Al^{3+}. It is significant to note that the difference of these peak currents is very small

with relative standard deviation value of 2.62%, indicating the good selectivity of GCMCNTs/GCE sensor.

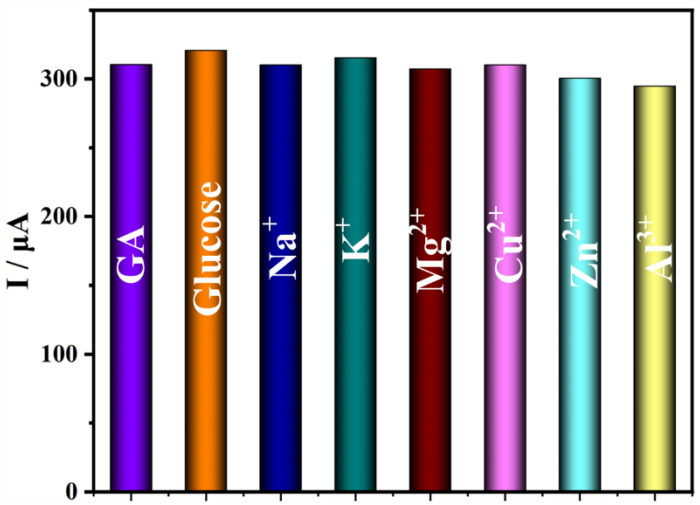

Figure 8. Selectivity of the GCMCNTs/GCE sensor for the GA detection (Parameters: pH=1, solution: 20 μM GA, deposition time: 100s).

3.8 Practical feasibility of GCMCNTs/GCE

The practical feasibility of GCMCNTs/GCE was studied in real tap water sample, which were filtered with the help of 0.22 μm filter and further spiked with MP solutions. **Table 2** lists the practical feasibility measurement result of MP at the GCMCNTs/GCE sample with different concentration (5, 7, 10 μm) in real tap water sample. As can be seen, the fabricated sensor exhibits satisfactory relative standard deviation values of 1.36-4.38 and recoveries of 96.15%-101.5%, indicating the good practical feasibility of GCMCNTs/GCE sensor.

Table 2. Practical feasibility of the GCMCNTs/GCE sensor for the GA detection in real tap water.

Sample	GA added (μM)	GA found (μM)	Recovery (%)	RSD (%)
Tap water	5	4.807	96.15	1.36
	7	6.951	99.30	3.83
	10	10.15	101.5	4.38

4. CONCLUSION

In this work, we successfully fabricated the GCMCNTs/GCE sensor for the GA determination. The fabricated sensor showed satisfactory detection performance towards GA with a low limit of detection of 0.0032 μM (S/N=3, GA concentration: 0.01-10 μM). The corresponding linear equation is

I_p (μA) =21.506C+3.134 (R^2=0.995), which can be attributed to the fact that GCMCNTs sample with high graphitization degree and carboxylation groups provided more microsites for electrochemical reaction and highly efficient electron transport channels. The GCMCNTs/GCE sensor also presented excellent practical feasibility for the GA detection in real tap water sample, which suggests the fabricated sensor has a good prospect in the field of GA detection.

ACKNOWLEDGMENTS
This work was financially supported by the Basic Research of Henan Institute of Science and Technology (No. 203010617011), and University Students' Innovation and Pioneering Project of Henan Institute of Science and Technology (No. 2022CX011).

References

1. H. Zhao, Q. Ran, Y. Li, B. Li, B. Liu, H. Ma, M. Zhang and S. Komarneni, *J. Mater. Res. Technol.*, 9 (2020) 9422.
2. B. Boye, E. Brillas, A. Buso, G. Farnia, C. Flox, M. Giomo and G. Sandonà, *Electrochimi. Acta*, 52 (2006) 256.
3. H.V.S. Ganesh, B.R. Patel, H. Fini, A.M. Chow and K. Kerman, *Anal. Chem.*, 91 (2019) 10116.
4. W. Ma, D. Han, S. Gan, N. Zhang, S. Liu, T. Wu, Q. Zhang, X. Dong and L. Niu, *Chem. Commun. (Camb)*, 49 (2013) 7842.
5. X. Tan, Q. Li and J. Yang, *Spectrochim Acta. A. Mol. Biomol. Spectrosc.*, 224 (2020) 117356.
6. J. Węgiel, B. Burnat and S. Skrzypek, *Diam. Relat. Mater.*, 88 (2018) 137.
7. C. Xiong, Y. Wang, H. Qu, L. Zhang, L. Qiu, W. Chen, F. Yan and L. Zheng, *Sensor. Actuat. B: Chem.*, 246 (2017) 235.
8. M. Chen, *Int. J. of Electrochem. Sci.*,14 (2019) 4852.
9. M. Ghaani, N. Nasirizadeh, S.A. Yasini Ardakani, F.Z. Mehrjardi, M. Scampicchio and S. Farris, *Anal. Methods*, 8 (2016) 1103.
10. K. Dhalwal, V.M. Shinde, Y.S. Biradar and K.R. Mahadik, *J. Food. Compos. Anal.*, 21 (2008) 496.
11. Natalia, Denderz, Jozef and Lehotay, *J. Chromatogr. A.*, 1372 (2014) 72.
12. Nunes, Salgado, Herida, Regina, Alencar, Fernandes, Felipe and Hugo, *Crit. Rev. Chem.*,46 (2016) 257.
13. W. Phakthong, B. Liawruangrath and S. Liawruangrath, *Talanta*, 130 (2014) 577.
14. Z. Sun, L. Zhao, L. Zuo, C. Qi, P. Zhao and X. Hou, *J. Chromatogr. B: Anal. Technol. Biomed. Life Sci.*, 958 (2014) 55.
15. Y.L. Su and S.H. Cheng, *Anal. Chim. Acta*, 901 (2015) 41.
16. S.M. Ghoreishi, M. Behpour, M. Khayatkashani and M.H. Motaghedifard, *Anal. Methods*, 3 (2011) 636.
17. R. Bavandpour, M. Rajabi, H. Karimi-Maleh and A. Asghari, *Microchem. J.*, 165 (2021) 106141.
18. X. Wang, Y. Xu, Y. Li, Y. Li, Z. Li, W. Zhang, X. Zou, J. Shi, X. Huang, C. Liu and W. Li, *Food. Chem.*, 357 (2021) 129762.
19. K. Prabhu, S.J. Malode and N.P. Shetti, *Environ. Technol. Inno.*, 23 (2021) 101687.
20. S. Đurđić, V. Stanković, F. Vlahović, M. Ognjanović, K. Kalcher, D. Manojlović, J. Mutić and D.M. Stanković, *Microchem. J.*, 168 (2021) 106416.
21. H. Huang, Y. Chen, Z. Chen, J. Chen, Y. Hu and J.J. Zhu, *J. Hazard. Mater.*, 416 (2021) 125895.
22. J.P. Winiarski, R. Rampanelli, J.C. Bassani, D.Z. Mezalira and C.L. Jost, *J. Food. Compos. Anal.*, 92 (2020) 103511.
23. K. Rajavel, M. Dinesh, R. Saranya and R.T.R. Kumar, *RSC. Adv.*, 5 (2015) 20479.

24. S. Zhang, Y. Shao, G. Yin and Y. Lin, *Appl. Catal. B-Environ.*, 102 (2011) 372.
25. M. Han, Z. Lv, L. Hou, S. Zhou, H. Cao, H. Chen, Y. Zhou, C. Meng, H. Du, M. Cai, Y. Bian and M.-C. Lin, *J. Power. Sources.*, 451 (2020) 227769.
26. Y. Xue, S. Zheng, Z. Sun, Y. Zhang and W. Jin, *Chemosphere*, 183 (2017) 156.
27. X. Li, M. Qu and Z. Yu, *Solid State Ionics*, 181 (2010) 635.
28. J. Balamurugan, A. Pandurangan, R. Thangamuthu and S.M. Senthilkumar, *Ind. Eng. Chem. Res.*, 52 (2013) 384.
29. A.T.E. Vilian, J.Y. Song, Y.S. Lee, S.K. Hwang, H.J. Kim, Y.S. Jun, Y.S. Huh and Y.K. Han, *Biosens. Bioelectron.*, 117 (2018) 597.
30. R. Abdel-Hamid and E.F. Newair, *J. Electroanal. Chem.*, 704 (2013) 32.
31. C.O. Chikere, N.H. Faisal, P. Kong Thoo Lin and C. Fernandez, *J. Solid. State. Electr.*, 23 (2019) 1795.
32. F. Gao, D. Zheng, H. Tanaka, F. Zhan, X. Yuan, F. Gao and Q. Wang, *Mater. Sci. Eng. C-Mater.*, 57 (2015) 279.
33. Y. Gao, L. Wang, Y. Zhang, L. Zou, G. Li and B. Ye, *Anal. Methods*, 8 (2016) 8474.
34. Z. Liang, H. Zhai, Z. Chen, H. Wang, S. Wang, Q. Zhou and X. Huang, *Sensor. Actuat. B-Chem.*, 224 (2016) 915.
35. J.H. Luo, B.L. Li, N.B. Li and H.Q. Luo, *Sensor. Actuat. B-Chem.*, 186 (2013) 84.
36. S.A. Shahamirifard, M. Ghaedi, Z. Razmi and S. Hajati, *Biosens. Bioelectron.*, 114 (2018) 30.
37. H. Liu, M. Hassan, X. Bo and L. Guo, *J. Electroanal. Chem.*, 849 (2019) 113378.
38. Y.L. Su and S.H. Cheng, *Anal. Chim. Acta*, 901 (2015) 41.
39. J. Tashkhourian and S.F. Nami-Ana, *Mater. Sci. Eng. C-Mater.*, 52 (2015) 103